Nuclear Instruments and Methods in Physics Research A 743 (2014) 114–120

Contents lists available at ScienceDirect

Nuclear Instruments and Methods in Physics Research A

journal homepage: www.elsevier.com/locate/nima

# Free-electron laser operation with a superconducting radio-frequency photoinjector at ELBE

J. Teichert [a,*], A. Arnold [a], H. Büttig [a], M. Justus [a], T. Kamps [b], U. Lehnert [a], P. Lu [a,c], P. Michel [a], P. Murcek [a], J. Rudolph [b], R. Schurig [a], W. Seidel [a], H. Vennekate [a,c], I. Will [d], R. Xiang [a]

[a] Helmholtz-Zentrum Dresden-Rossendorf, Bautzner Landstr. 400, 01328 Dresden, Germany
[b] Helmholtz-Zentrum Berlin, Albert-Einstein-Str. 15, 12489 Berlin, Germany
[c] Technische Universität Dresden, 01062 Dresden, Germany
[d] Max-Born-Institut, Berlin, Max-Born-Str. 2a, 12489 Berlin, Germany

ARTICLE INFO

*Article history:*
Received 31 May 2013
Received in revised form
30 July 2013
Accepted 6 January 2014
Available online 17 January 2014

*Keywords:*
Superconducting RF
SRF gun
Photo injector
Free-electron laser

ABSTRACT

At the radiation source ELBE a superconducting radio-frequency photoinjector (SRF gun) was developed and put into operation. Since 2010 the gun has delivered beam into the ELBE linac. A new driver laser with 13 MHz pulse repetition rate allows now to operate the free-electron lasers (FELs) with the SRF gun. This paper reports on the first lasing experiment with the far-infrared FEL at ELBE, describes the hardware, the electron beam parameters and the measurement of the FEL infrared radiation output.



## 1. Introduction

High-brightness electron sources for CW operation with megahertz pulse repetition rates and bunch charges up to 1 nC are still a topic for research and development. One promising approach is a superconducting radio-frequency photoelectron injector (SRF gun). Similar in the basic design to a traditional RF photoelectron injector, the SRF gun has a superconducting niobium cavity instead of a copper RF cavity. Therefore the SRF gun can combine the high brightness of normal conducting RF photo guns with the advantages of superconducting RF, i.e. low RF losses and CW operation. Proposed by Chaloupka and co-workers [1] in 1988, the first experimental set-up was installed at the University of Wuppertal [2]. Later, the first electron beam from an SRF gun with a half-cell 1.3 GHz cavity was produced at FZR (now HZDR) by Janssen and co-workers [3] in 2002. The work has been continued by developing and commissioning a 3½-cell SRF gun for the ELBE accelerator [4]. At present, SRF gun research and development programs are conducted in a growing number of institutes and companies like AES, Peking University, BNL, DESY, HZB, HZDR, Niowave, NPS, TJNAF, and Wisconsin University. (Ref. [5] gives a detailed overview.) Several recently launched accelerator-based light source projects plan the application of SRF guns [6–8].

The radiation source Electron Linac of high Brilliance and low Emittance (ELBE) at the Helmholtz-Zentrum Dresden-Rossendorf (HZDR) is a user facility and operates two infrared free-electron lasers (FELs) for several years now [9–11]. The undulators of the two FELs have period lengths of 27.3 mm (U27), and 100 mm (U100) respectively and produce radiation in the wavelength range between 4 and 250 μm. The distinctive feature of ELBE is its continuous wave (CW) operation. Fitting them to the optical resonator lengths of the FELs of 11.53 m, electron bunches with a repetition rate of 13 MHz can be generated within uninterrupted trains. Additionally to the FELs the ELBE electron beam is used to generate various kinds of secondary radiation like gamma rays, positrons, and neutrons. Each of the two main radio-frequency (RF) accelerator modules of the ELBE linac contains two superconducting cavities. The cavities are kept at 2 K using superfluid helium delivered by a helium liquefier. The design of the 9-cell, 1.3 GHz cavities was developed for the TESLA project at DESY [12] and the maximum acceleration field is specified to 10 MV/m giving a maximum total energy of 40 MeV.

Since the commissioning of ELBE, the electron beam has been generated by means of a thermionic electron source with dispenser cathode and pulsing grid. A high-voltage of 235 kV is applied to this gun. Two RF bunchers compress the pulse length of 500 ps at the exit of the source to about 10 ps (FWHM values) at

* Corresponding author. Tel.: +49 3512603445; fax: +49 3512603690.
*E-mail address:* j.teichert@hzdr.de (J. Teichert).

0168-9002/$ - see front matter © 2014 Elsevier B.V. All rights reserved.
http://dx.doi.org/10.1016/j.nima.2014.01.006

the linac's entrance. Although very reliable for user operation, the source has the disadvantages that the bunch charge is limited to 80 pC, and that the transverse emittance is reaching about 12 mm mrad rms at this bunch charge.

The ELBE SRF gun is able to inject an electron beam into the linac using a dogleg-like connection beamline since 2010 [13]. In 2012 a new ultraviolet (UV) driver laser for the SRF gun was installed which had been developed at the Max-Born-Institut by Will and co-workers [14]. This laser fulfills the specification for the planned user application and is able to deliver pulses with 13 MHz (ELBE FEL mode) as well as lower repetition rates (500, 250, and 100 kHz) for high-charge operation. The new laser allows applying the SRF gun for the FEL operation at ELBE. In this paper we will report on the first successful attempt of this procedure. It is worth to mention that the SRF gun at ELBE is still the only one of this type which delivers beam to an accelerator and furthermore this is the first demonstration of FEL lasing with such a gun at all.

## 2. SRF gun

A schematic design view of the SRF gun is presented in Fig. 1. The cryomodule contains the superconducting cavity, tuners, helium tank, liquid $N_2$-vessel with cryogenic shield, magnetic shielding, photocathode with support and cooling system, higher-order-mode couplers, main power coupler, and further diagnostics and auxiliary systems. The 1.3 GHz niobium cavity consists of three TESLA cells [12] and a specially designed half-cell. At the cathode side of the cavity an additional choke cell, also superconducting, prevents the leakage of the RF field of the cavity towards the cathode support system. Details of the SRF gun design have been published in [4].

The normal conducting photocathode is installed in a special support system, which is isolated from the superconducting cavity by a vacuum gap and cooled with liquid nitrogen. This design allows the application of semiconductor photocathodes of high quantum efficiency. Up to now $Cs_2Te$ photo cathodes have been used. This material has both high quantum efficiency (QE) and robustness against vacuum deterioration [15]. One of the SRF gun related questions is how to guarantee the compatibility of the normal conducting cathode and the superconducting cavity. The operation experience is that the photocathodes have lifetimes of months and relatively stable QE [16]. That is at least true for the previous operation conditions of the gun with a typical laser power of 0.5 W, a laser power density of less than 1 W/mm$^2$, and pulse energies up to 10 μJ. Before the FEL experiment, the gun produced an average current up to 0.5 mA with the same photo cathode and the total charge extracted was 200 As so far.

The second question is whether the photo cathode operation degrades the superconducting cavity over time. Therefore the cavity performance, i.e. the intrinsic quality factor $Q_0$ versus the peak electric field, has been measured regularly since the commissioning of the gun in 2007. Fig. 2 shows some results of these measurements. The practical limitation for the peak field value of the acceleration field in the present cavity is the $Q_0$ decrease and the corresponding increase of the RF heat loss in the cavity surface. For higher fields the source is the strong field emission. The acceptable heat loss is about 30 W. From 2007 until 2011 the values for the peak fields were 16 MV/m in CW and 21.5 MV/m for pulsed RF. (3 MeV and 4 MeV kinetic energy, respectively.) A temporary increase was obtained by high power processing (HPP) of the cavity. In autumn 2011 a number of photocathodes were exchanged within a short time for testing new designs and

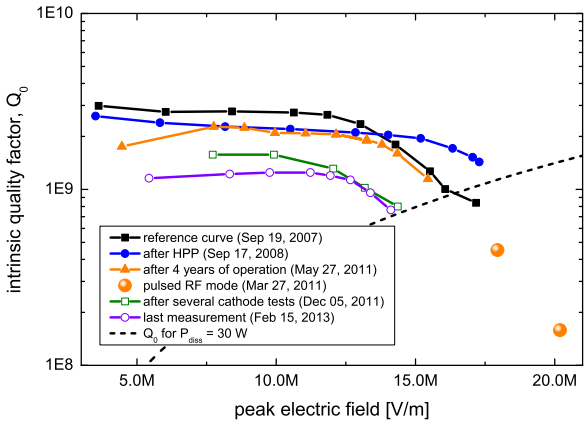


**Fig. 2.** Measurement of the cavity performance.

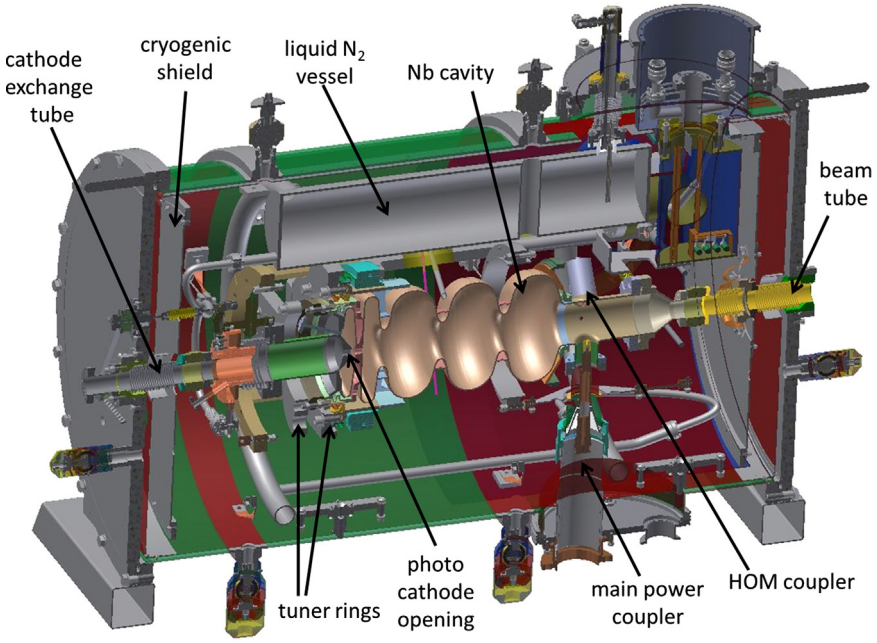


**Fig. 1.** Cross-section CAD drawing of the 3½-cell SRF gun cryomodule.

materials, as well as vacuum repair work was carried out at the beamline near the SRF gun. The measurement carried out afterwards (December 2011) showed a performance decrease of 12%. But no further deterioration has been observed up to the present. Our experience is that the photocathode operation does not lower the gun cavity performance, but the cathode exchange is a critical issue.

For the first lasing, the SRF gun was operated with pulsed RF. This allowed a higher acceleration gradient at low RF losses into the helium path and thus a more stable operation at higher exit energy. The RF pulse consisted of a ramping time with increasing gradient and a macropulse time, in which the gradient and phase are stabilized and the beam can be produced. These times were fixed to 12 ms and 6 ms, respectively. The repetition period of the RF pulses was chosen to be 800 ms. The acceleration gradient was $E_{acc}=6.6$ MV/m which corresponds to a peak field of $E_{peak}=18$ MV/m ($E_{peak}=2.7\times E_{acc}$) and yields 3.3 MeV kinetic energy at the gun exit.

During the ramp-up time of the RF, multipacting appeared in the coaxial channel formed by the hole in the backplane of the half-cell and the photocathode. To suppress this effect, a distinct DC voltage is applied to the photo cathode. For pulsed operation this voltage has to be present all the time and was chosen to be $-5.3$ kV with respect to the grounded cavity.

The driver laser consists of a Nd:glass oscillator at 52 MHz, a pulse picker generating the 13 MHz with an electro-optical modulator, a fiber-laser preamplifier, a multipass amplifier, and a frequency conversion stage with lithium triborate (LBO) and beta-barium borate (BBO) crystals. The UV laser pulse had a Gaussian shape in time with a FWHM value of about 3 ps. The transverse profile can be shaped with a variable aperture. Here the aperture was completely opened in order to obtain maximum laser pulse energy. Thus, the transverse profile was also Gaussian with 1.2 mm FWHM. The UV laser power on the laser table was measured as 600 mW. Considering the transportation losses of 50%, the laser pulse energy at the photocathode was about 23 nJ. The laser pulse train period was varied between 0.5 and 2 ms (6500 to 26000 micro pulses).

The laser spot was centered on the photocathode and the laser parameters were optimized to maximize the electron current. A value of 260 μA which corresponds to a bunch charge of 20 pC was obtained und held stable during the whole beam time.

The photocathode plug was made of Mo polished to a roughness of 8 nm. A $Cs_2Te$ photo emission layer of 4 mm diameter was deposited on top by successive evaporation of Te and Cs in an ultra-high-vacuum preparation system [16]. The photocathode was prepared 12 months ago with a fresh QE of 8.5%, while a recent measurement has shown 0.6%. During the gun set-up, the electron current was measured with a retractable Faraday cup in front of the gun. This signal was used to calibrate a stripline beam position monitor (sum signal) which served for noninvasive current monitoring during the whole beam time.

The driver laser phase, which determines the time when the laser pulse hits the cathode, was set to $-5^\circ$. The definition is in such a way that for the zero-point the center electron in the bunch exits the photocathode at the zero-crossing of the RF field: $F_e=e(E_{DC}(0)-E_{RF}(0)sin\varphi_l)$. Thereby $F_e$ represents the force on the electron, $e$ is the (negative) electron charge, $E_{DC}(0)$ is the DC field strength at the cathode, and $E_{RF}(0)$ is the RF field amplitude at the cathode. A typical laser phase scan measured with the same gun parameters as mentioned above, but with slightly lower beam current is shown in Fig. 3. Due to the cathode's DC field, electron beam emission starts at negative laser phases. The phase window with nearly constant beam current reaches up to 60°. The upper limit is due to phase mismatch of the bunch in the full cavity cells, i.e. the electrons start too late to be accelerated. In general, the beam quality is better for a small laser phase. As an example, the dependences of the beam energy and energy spread on the laser phase are presented in Fig. 4. These measurements were done with a 180° bending magnet in the SRF gun diagnostic beamline [17]. The transverse emittance has a similar dependency, but was not determined during this experiment. An earlier measurement using the slit scan method delivered a value of 1 mm mrad for the normalized rms emittance. The relevant parameters like acceleration gradient, laser phase, and laser spot size were the same as in the present gun setup.

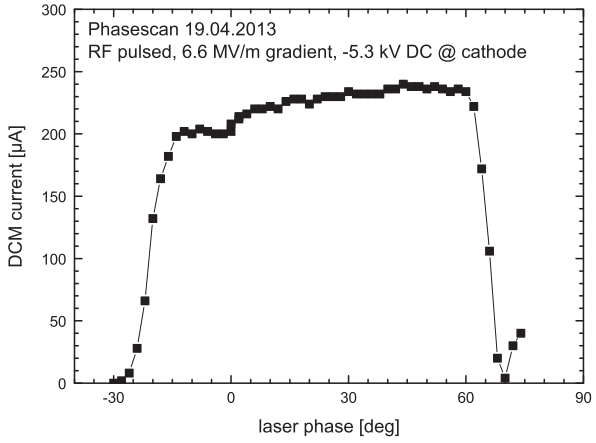


**Fig. 3.** Phase scan of the laser with respect to the gun RF phase. The current maximum corresponds to 18 pC.

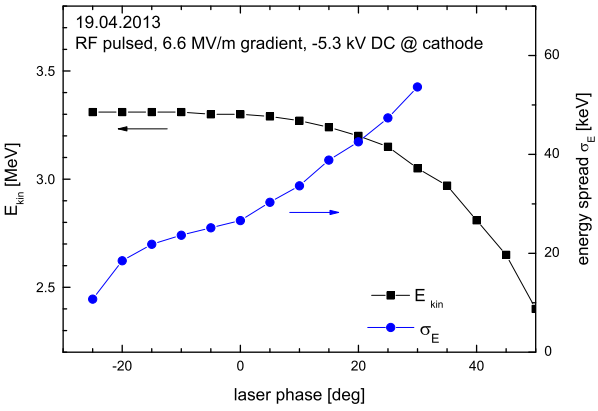


**Fig. 4.** Kinetic energy and rms energy spread versus laser phase. The bunch charge was 18 pC (240 μA beam current in the macro pulse).

## 3. Accelerator

The beamline layout with the SRF gun, dogleg, accelerator, *S*-bend, and FEL is presented in Fig. 5. Starting with 3.3 MeV at the SRF gun exit, the electrons were accelerated to 16 MeV in the first ELBE module (cavities C1 and C2) and up to the final energy of 27.9 MeV in the second ELBE module (cavities C3 and C4). Viewscreens were utilized for steering the beam exactly. In Fig. 5 they are indicated in black color. There are different types in use: Ce-doped yttrium aluminum garnet (YAG) screens in the diagnostic beamline and in the dogleg, alumina screens in the straight section before ELBE module 1, and optical transition radiation (OTR) screens made of Al foil at all positions after module 1. At a number of places stripline monitors detected the beam current and helped to sustain full transmission. A loss-free and achromatic beam transport in the dogleg section was essential for the success. After

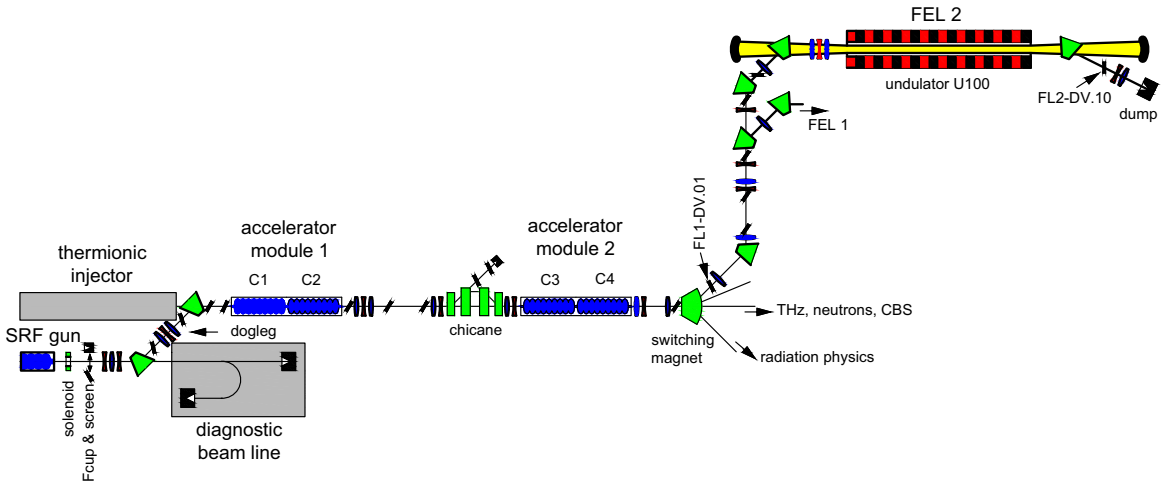


**Fig. 5.** Beamline for FEL operation with SRF gun.

**Table 1**
FEL U100 operating parameters.

| *Parameter* | *Notation* | *Value* |
|---|---|---|
| *Electron beam* | | |
| Energy | $E$ | 27.9 MeV |
| Bunch charge | $Q$ | 20 pC |
| RMS bunch length | $\sigma_t$ | 1.6 ps |
| Normalized transverse emittance | $\varepsilon_n$ | 1 mm mrad |
| Repetition frequency | $f$ | 13 MHz |
| RMS energy spread | $\sigma_E$ | 24 keV |
| Macropulse duration | $t_{MP}$ | 0.5–2 ms |
| Macropulse repetition rate | $f_{MP}$ | 1.25 Hz |
| *Undulator* | | |
| Type | | Hybrid planar, SmCo magnets |
| Period | $\lambda_U$ | 100 mm |
| Number of periods | $N$ | 38 |
| Undulator parameter | $K_{rms}$ | 0.3–2.7 |
| *Optical cavity* | | |
| Type | | Partial waveguide |
| Cavitylength | $L$ | 11.53 m |
| Rayleigh length | $R$ | 1.8 m |
| Mirror material | | Cu/Au |
| Outcoupling | | Holes 2.0, 4.5, 7.0 mm |

**Table 2**
Longitudinal electron bunch parameters.

| *Parameter* | *Notation* | *Lasingsetting* | *Gun/doglegexit* |
|---|---|---|---|
| RMS energy spread | $\sigma_E$ | 24.1 keV | 33.9 keV |
| RMS bunch length | $\sigma_t$ | 1.54 ps | 1.60 ps |
| Longitudinal emittance $\varepsilon_n$ | $\varepsilon_L$ | 36.6 keV ps | 44.1 keV ps |
| Correlation parameter | $r_{12}$ | 0.19 | −0.58 |
| Correlated energy spread | | 4.5 keV | −19.7 keV |
| RMS slice energy spread | | 23.8 keV | 27.5 keV |

achieving that, the phases of the linac cavities were matched and the final energy adjusted. Finally, the steering and focusing in the S-bend and undulator section were carried out. Table 1 gives a summary of parameters concerning the electron beam and the FEL hardware.

The energy chirp of the electron bunch after the gun and the dogleg was negative, i.e. the electrons in the head of the bunch had higher energy than those in the tail. In the first cavity C1 this correlated energy spread was compensated for by setting the RF phase about 20° off crest. The following cavities C2–C4 were operated on-crest. The magnetic bunch compressor (chicane) between the two ELBE modules was not used. The *S*-band from the switching magnet to the undulator U100 has a positive momentum compaction coefficient of $R_{56}=93$ mm. (In the convention used here a magnetic bunch compressor has the opposite sign, i.e. $R_{56}<0$ and the head of the bunch is at $z=ct<0$.) Thus, the S-bend could shorten the bunch in case it had a negative energy chirp. But due to the compensation of the correlated energy spread with cavity C1, the bunch length was unchanged and had the same value as initially created in the SRF gun.

In the last part of the beam time available for this experiment, the longitudinal phase space parameters in the linear approximation were measured. These parameters define the bunch length, correlated energy spread, and the slice energy spread. The applied method was the phase scan technique, described in [18]. This means the RF phase of cavity C4 was varied while the beam energy spectrum was measured using the dipole magnet downstream the ELBE module 2 and the first screen right behind it (screen FL1-DV.01 in Fig. 5).

As mentioned above, the cavities C2–C3 were on crest in this particular accelerator setup. Therefore, they did not alter the longitudinal phase space and C4 could be used for the measurement. In the second measurement series, the C1 phase was set on crest too. In this case the data delivers the phase space as produced by the SRF gun itself. Both results are presented in Table 2, while the phase space plots are shown in Fig. 6. It can be seen that the energy correlation was slightly overcompensated in the lasing setting giving a correlation parameter of 0.19. The bunches delivered by the gun itself had a correlated energy spread of 20 keV and a correlation parameter of -0.58. The rms bunch length was measured to 1.6 ps with good agreement between both measurements. For the rms longitudinal emittance with a value of about 40 keV ps, the difference is larger and mainly caused by the simple measurement setup with a high background. An existing Browne Buechner spectrometer [19] would allow for a more accurate analysis, but was not available due to ongoing beamline reconstruction.

## 4. FEL

The U100 FEL for radiation in the far infrared range from 18 to 250 μm is based on a SmCo hybrid undulator which is composed of 38 magnet periods each 100 mm long. The $K_{rms}$ can be adjusted from 0.3 to 2.7, which corresponds to gaps of 85 to 24 mm. The FEL is equipped with switchable outcoupling mirrors (three different

hole diameters of 2, 4.5, and 7 mm). In order to obtain sufficient magnetic fields in the undulator, the gap and consequently the place for the optical mode has to be adequately small. Therefore, the U100 FEL is equipped with a partial parallel-plate waveguide with 10 mm height [20]. The horizontal size is wide enough to allow free propagation. The waveguide spans from the undulator entrance to the downstream mirror. In the remaining part of the optical cavity the optical mode propagates freely.

The mirrors are toroidal at the free propagation side (6.33 m and 3.61 m radius of curvature) and cylindrical (6.33 m curvature) at the waveguide side. They are made of copper with gold coating. The resonator has to be set and stabilized to a certain length and its axis has to be aligned to the fixed apertures. For this purpose the mirrors are gimbal-mounted and can be tilted horizontally and vertically by means of piezoelectric drives. Moreover the downstream mirror can be shifted along the resonator axis by 10 mm in steps of 100 nm by means of remote controlled DC drives. The electron beam has to be aligned to this fixed resonator axis. An interferometer system is used for monitoring the resonator length. Furthermore, there is an extensive beam diagnostics system at the FEL consisting of 20 view-screens, markers, and auxiliary mirrors.

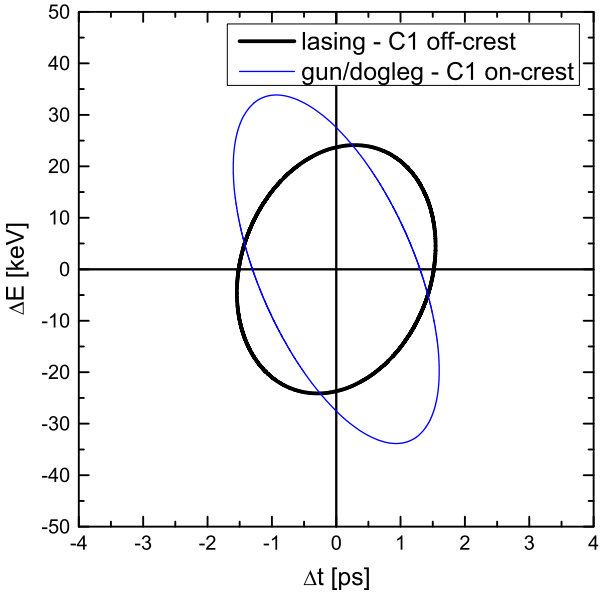


**Fig. 6.** Longitudinal phase space ellipses for the 20 pC beam measured with the phase scan technique. It shows the ellipse for the lasing setting with nearly compensated correlated energy spread (C1 off-crest), and in the ellipse as produced by the gun with a negative correlated energy spread (C1 on-crest).

The insertion units are OTR screens made of beryllium with a 1 mm hole, foil screens consisting of a stretched aluminum foil, and markers with a hole for the resonator mirror alignment and for the interferometer lasers. CCD cameras in lead housings are used to observe the screens and markers.

The infrared light produced by the FEL is guided into the diagnostics room. There are several detectors: Mercury Cadmium Telluride (MCT) detectors for shorter and pyroelectric detectors for longer wavelengths. A multichannel spectrometer serves for wavelength, and two power meters for intensity measurements. By means of a switching mirror system, the FEL beam can be distributed from the diagnostic room to the different user laboratories.

The FEL 2 with the Undulator U100 is designed for the ELBE linac utilizing the thermionic injector. Stable production of far IR radiation requires an electron energy between 20 and 40 MeV with an energy spread less than 60 keV, an bunch length less than 4 ps, a bunch charge of more than 50 pC (about 10 A peak current), and an alignment accuracy of the electron beam with respect to the undulator axis of 0.2 mm. According to the relative high emittance of the thermionic source, the requirement is a normalized transverse emittance of less than 15 mm mrad [21]. Using the SRF gun, the parameters for transverse emittance, energy spread, and bunch length are not critical. The crucial point was the small bunch charge which was lower than the design specification. Here the shorter bunch length helped to achieve the necessary peak current.

For the experiment reported here, the undulator gap was set to produce radiation of 41.5 μm wavelength, which corresponds to an undulator gap of 50.8 mm. Later, the gap was changed to 46.2 mm. The mirror with the smallest out-coupling hole (2 mm) was chosen. The adjustment of the optical mirror axis was checked and the electron beam guided through the undulator by means of the OTR screens. Finally, the optical cavity length was scanned. To find the onset of lasing, the infrared pyroelectric detector signal and the electron beam spot image on the screen in the dispersive section behind the deflecting magnet (screen FL2-DV.10 in Fig. 5) were observed. Here a distinct increase of the electron energy spread was expected.

Indeed, after a small variation of the optical cavity length lasing was observed. Fig. 7 shows the OTR screen picture of the electron beam before and during FEL lasing with the expected increased energy width. The first measured detuning curve of the FEL is shown in Fig. 8 while the infrared spectrum is presented in Fig. 9. The width of the peak was measured to be 1 μm FWHM. Under the assumption that the infrared pulses are transform limited, the time-bandwidth product is one half: $\Delta\nu\Delta t = 1/\lambda(\Delta\lambda/\lambda)\Delta z \approx 0.5$. This yields $\Delta t \approx 0.5\lambda^2/(c\Delta\lambda)$ and allows an estimation of the optical

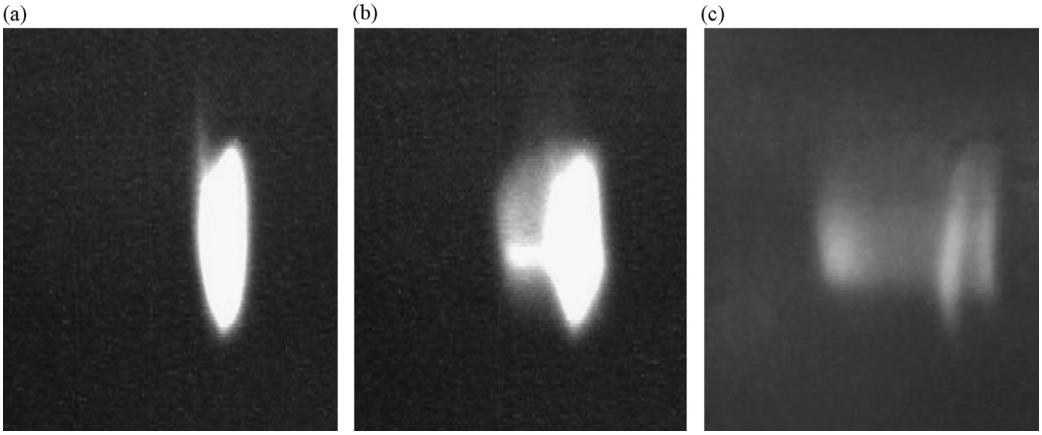


**Fig. 7.** Screenshots with the electron beam in the dispersive section behind the FEL: (a) before lasing, (b) first lasing, (c) lasing with optimized beam transport in undulator.

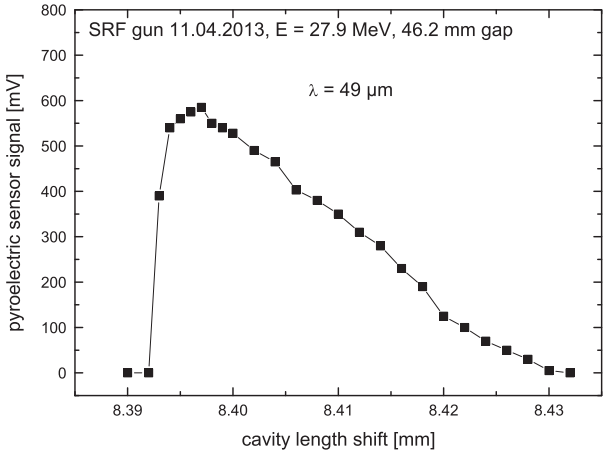


**Fig. 8.** Measured FEL detuning curve for 49 μm wavelength. The length scale is the relative downstream mirror position. Zero detuning length is nearly located at the left-side slope of the curve.

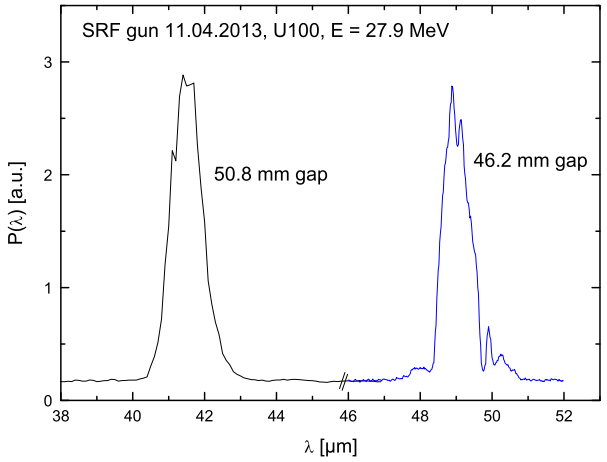


**Fig. 9.** First measured FEL infrared spectra for undulator gaps of 50.8 and 46.2 mm.

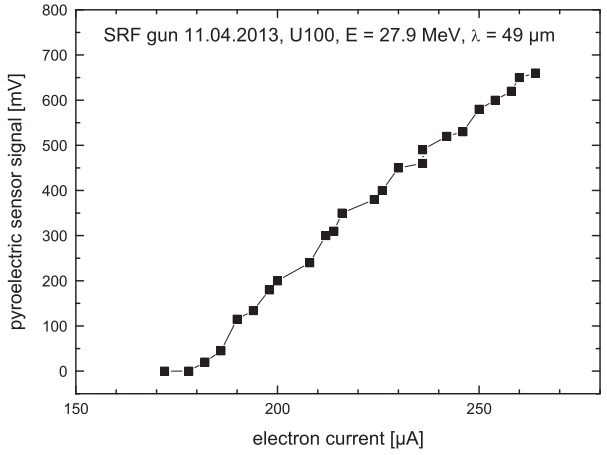


**Fig. 10.** Electron current dependence of FEL power.

pulse length. The result is 4 ps FWHM, which is slightly longer than the electron bunch length. This value was measured near the maximum in the FEL detuning curve, i.e. it belongs to a small detuning. For a larger detuning the FEL pulses should become longer while the bandwidth gets smaller.

In Fig. 10 the FEL output power (amplitude of the pyroelectric sensor signal) as a function of the electron beam current is

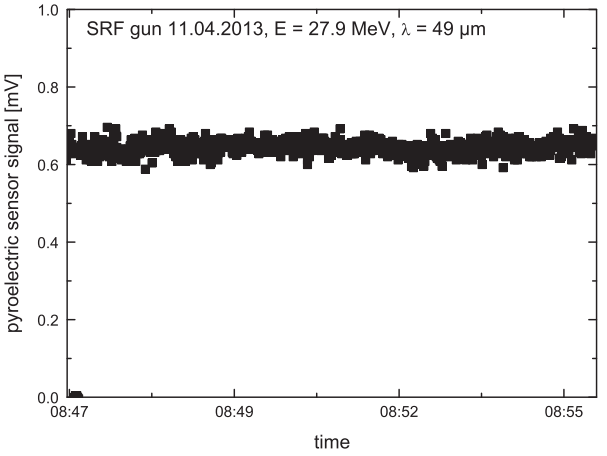


**Fig. 11.** Stability of FEL output power.

depicted. There is a clear linear dependence. The lower limit for lasing was an electron current of 180 μA. The upper limit of 260 μA belonged to the maximum electron current of the gun, which was determined by the laser power and the QE of the photocathode. A very rough estimation from the value of the power meter, which was not suitable for the low macropulse repetition rate, delivered a laser power of 2 W in the macropulse. This value is much lower than the power of a standard CW operation with the thermionic injector. But in that case the electron current is typically 600–800 μA. The stability of the FEL output power was measured over an adequate time. A stability plot over 10 min is presented in Fig. 11. The result which delivers an amplitude variance value of 12%, is similar to the one for FEL operation with the thermionic injector.

## 5. Conclusion and future plans

The operation of a FEL requires a comparably high level of beam quality with respect to all kinds of stabilities like beam energy, bunch charge, transverse position, phase jitter etc. Thus, successful lasing with the SRF gun represents an important milestone and confirms the design concept for this gun and the applicability in accelerator facilities.

The long-term experience with normal-conducting, semiconductor photocathodes is promising. The operational lifetime is months and average currents up to 0.5 mA have been produced. For the cavity performance we have not seen any degradation which is due to the operation of the gun. A decrease of 12% in cavity performance is likely caused by cathode exchange or beamline vacuum work.

The SRF gun is still in its research and development phase, and it is not intended to apply the gun for standard user operation instead of the thermionic injector. However, there are some user requests for specific FEL operation parameters which cannot be realized with the thermionic injector. One interesting operation mode, which could be supported by the SRF gun in near future, is a macropulse operation with 1 kHz and nearly 50% duty cycle. Here the requirements for the SRF gun are RF operation in CW, realization of a high average current – at least 500 μA in the macropulse – and a stable operation with this current maintaining low beam loss.

In the medium term future, the present SRF gun will be replaced by an upgraded version. The progress will include an improved superconducting cavity with significantly better performance than the present gun cavity. This will allow much higher acceleration gradients (40 MV/m peak field) and an exit electron

kinetic energy up to 8 MeV. The benefit from this is also an improved beam quality, i.e. lower transverse emittance and energy spread, which will simplify the beam transport through the dogleg section. FEL enhancements could benefit from the higher beam energy available due to the higher entrance energy into ELBE and the full energy gain in the first cavity. Here the $\beta < 1$ injection with the thermionic injector causes a loss of about 3 MeV. The higher energy would allow lasing at shorter wave length with the U100 FEL, and thus close the gap between the U27 and U100. The lower transverse emittance results in a transversally smaller beam in the undulator, which could increase the gap range without additional focusing adjustment, and thus widen the wavelength range in spectral measurements.

## Acknowledgements

We would like to thank the whole ELBE team for their help and assistance with this project. Especially we would like to thank J. Fiedler, E. Kraft, and O. Pfützner for their strong support during the measurement shifts. The work is supported by the European Community - Research Infrastructure Activity under the FP7 programme (EuCARD, contract number 227579), and by the German Federal Ministry of Education and Research grant 05 ES4BR1/8.

## References

[1] H. Chaloupka, et al., Nuclear Instruments and Methods A 285 (1989) 327.
[2] A. Michalke, Ph.D. thesis, University of Wuppertal, 1992, WUB-DIS 92-5.
[3] D. Janssen, et al., Nuclear Instruments and Methods A 507 (2003) 314.
[4] A. Arnold, et al., Nuclear Instruments and Methods A 577 (2007) 440.
[5] A. Arnold, J. Teichert, Physical Review Special Topics – Accelerators and Beams 14 (2011) 024801.
[6] A. Jankowiak, et al., Proceedings of LINAC10, Tsukuba, Japan, 2010, p. 407.
[7] R.A. Bosch, et al., Proceedings of FEL09, Liverpool, UK, 2009, p. 651.
[8] S.P. Niles, et al., Proceedings of FEL10, Malmö, Sweden, 2010, p. 457.
[9] P. Michel, et al., Proceedings of FEL04, Trieste, Italy, 2004, p. 8.
[10] P. Michel, et al., Proceedings of FEL06, Berlin, Germany, 2006, p. 488.
[11] W. Seidel, et al., Proceedings of FEL08, Gyeongju, Korea, 2008, p. 382.
[12] B. Aune, et al., Physical Review Special Topics – Accelerators and Beams 3 (2000) 092001.
[13] J. Teichert, et al., Proceedings of FEL10, Malmö, Sweden, 2010, p. 453.
[14] I. Will, et al., will be published.
[15] L. Monaco, et al., Proceedings of PAC07, Albuquerque, USA, 2007, p. 2763.
[16] R. Xiang, et al., Proceedings of IPAC12, New Orleans, USA, 2012, p. 1524.
[17] T. Kamps, et al., Review of Scientific Instruments 79 (2008) 093301.
[18] D.H. Dowell, et al., Nuclear Instruments and Methods A 507 (2003) 331.
[19] J. Rudolph, et. al., Proceedings of DIPAC11, Hamburg, Germany, 2011, p. 416.
[20] M. Freitag, et al., Proceedings of FEL06, Berlin, Germany, 2006, p. 345.
[21] R. Wünsch, Annual Report 2003/04 – Radiation Source ELBE, FZR-428, 2005, p. 67, ⟨http://www.hzdr.de/publications/007356/7356a.pdf⟩.